ADVANCED MATERIALS

Supporting Information

Giant Thermal Expansion in 2D and 3D Cellular Materials

Hanxing Zhu,* Tongxiang Fan, Qing Peng, and Di Zhang

Supporting Information

Giant Thermal Expansion in 2xD and 3D Cellular Materials

By *Hanxing Zhu* [a,*]*, Tongxiang Fan* [b]*, Qing Peng* [c, d] *and Di Zhang* [b]

[a] School of Engineering, Cardiff University, Cardiff, CF24 3AA, UK

[b] State Key Lab of Metal Matrix Composites, Shanghai Jiaotong University, Shanghai, 200240, China

[c] School of Power and Mechanical Engineering, Wuhan University, Wuhan 430072, China.

[d] Nuclear Engineering and Radiological Sciences, University of Michigan, Ann Arbor, Michigan 48109, United States

∗ Corresponding author: H.X.Z. (zhuh3@cf.ac.uk)

S1. Thermal Expansion in the first level cellular materials

All types of the 2D and 3D cellular materials shown in Figures 1 and 2 are assumed to be made of two different solid ingredients A and B. Ingredient A is chosen as a ceramic with a Young's modulus of $E_A = 2 \times 10^{11}$ N/m^2 and a thermal expansion coefficient of $\alpha_A = 3 \times 10^{-6}$ K^{-1}, and ingredient B is chosen as a polymer with a Young's modulus of $E_B = 3 \times 10^9$ N/m^2 and a thermal expansion coefficient of $\alpha_B = 200 \times 10^{-6}$ K^{-1}. All the non-straight struts are assumed to have the same chevron shape with a span of $L = 1.0$ and an amplitude of a, and to be pin-connected with the straight struts of the cross in the middle of the RVEs. In addition, all the chevron struts are assumed to have the same uniform thickness t for 2D cellular materials or the same uniform square cross-section of side t for 3D cellular materials. Moreover, all the dimensions in Figures 1-3, including the *x, y* and *z* axes, are normalized by L. It is noted that the geometrical structure of ingredient B in Fig. 1c is similar to the 4-star auxetic honeycomb[31].

S1.1. Small linear deformation analysis of chevron struts

A temperature increase ΔT can result in a compressive force P at the two ends of the chevron struts due to the thermal mismatch between the chevron struts and the cross in the middle of the RVEs, as illustrated in Figure 3a. Small deformation analysis is based on the initial configuration of the structure, the axial compressive strain in the longitudinal direction of the chevron struts can thus be obtained as

$$\varepsilon = \frac{P\cos\theta}{E_B A} \tag{S1-1}$$

Where E_B is the Young's modulus of ingredient B and A is the cross-sectional area of the chevron struts. Obviously, the magnitude of the axial compressive strain ε can't be larger than the relative thermal strain of the chevron struts $\Delta\alpha\Delta T = (\alpha_B - \alpha_A)\Delta T$. If $\alpha_B = \alpha_A$, the thermal expansion coefficients of all different types of the first level 2D and 3D cellular materials shown in Figures 1 and 2 would be the same as α_A. It is noted that all the straight struts of the cross in the middle of the 2D and 3D RVEs undergo uniaxial tension (or compression) due to the structural symmetry. Thus, the effects of their tensile deformation on the thermal expansion are negligible because $E_A \gg E_B$.

Taking account the combined effects of thermal expansion and bending, axial compression and transverse shear of the chevron struts, according to the symmetry, the following deformation compatibility condition in the longitudinal direction of half a chevron strut in Fig. 3a must be satisfied[32].

$$\frac{[\frac{L}{2\cos\theta}(1+\Delta\alpha\Delta T - \varepsilon)]^3 P\sin\theta}{3E_B I}\tan\theta + \frac{1.2\times 2(1+v_B)}{E_B A}(\frac{L}{2\cos\theta})(P\sin\theta)\tan\theta = (\Delta\alpha\Delta T - \varepsilon)\frac{L}{2\cos\theta} \tag{S1-2}$$

Where $\Delta\alpha\Delta T$ is the relative thermal strain of the chevron strut and ε given by (S1-1) is the axial compressive strain in the longitudinal direction of the chevron struts, I is the second moment of the cross-sectional area of the chevron struts, the Poisson ratio v_B of ingredient B (i.e. polymer) is taken as 0.5 and the transverse shear coefficient of the square cross-section of the chevron struts is 1.2. In Eq. (S1-2), the first and second terms on the left hand side are associated to beam bending and transverse shear deformation[32], respectively, and the term on the right hand side is the elongation of half a chevron strut in its longitudinal direction due to thermal expansion and axial compression. Substituting Eq. (S1-1) into Eq. (S1-2) leads to

$$c_1(1+\Delta\alpha\Delta T-\varepsilon)^3\varepsilon+c_2\varepsilon=\Delta\alpha\Delta T-\varepsilon \tag{S1-3}$$

Where $c_1=\dfrac{Aa^2(L^2+4a^2)}{3IL^2}$ and $c_2=\dfrac{14.4a^2}{L^2}$. Equation (S1-3) indicates that the magnitude of the axial compressive strain ε in the longitudinal direction of the chevron struts is a nonlinear function of c_1, c_2 and $\Delta\alpha\Delta T$.

For given values of c_1, c_2 and $\Delta\alpha\Delta T$, ε can be solved from Eq. (S1-3) using the Newton-Raphson method, and the change of the amplitude of the chevron struts can be obtained as

$$\Delta a=\frac{L(\Delta\alpha\Delta T-\varepsilon)}{2\sin\theta\cos\theta}=\frac{L^2+4a^2}{4a}(\Delta\alpha\Delta T-\varepsilon) \tag{S1-4}$$

For the first level 2D cellular materials with pin-connections between the chevron struts and the cross in the middle, as shown in Figure 1c, the total change of the dimensionless size of the RVE due to the combined effects of temperature change ΔT and the resultant internal force P can be obtained as

$$\Delta_{RVE}=-2\Delta a+\alpha_A\Delta T+2(a+b)\alpha_B\Delta T \tag{S1-5}$$

3

From the dimensionless dimensions given in Figure 1c, the isotropic negative linear thermal expansion coefficient (NTEC) of the first level 2D cellular material can be derived as

$$\alpha_1 = \alpha_{RVE} = \frac{\Delta_{RVE}}{(1+2b)\Delta T} = \frac{\alpha_A + 2(b-a)\alpha_B}{1+2b} - \frac{2\Delta a}{(1+2b)\Delta T} \approx -\frac{1.667\Delta a}{\Delta\alpha\Delta T}\Delta\alpha = -k_1\Delta\alpha \qquad (S1\text{-}6)$$

Where the dimensionless value of $b = b/L$ is chosen as 0.1, and Δa is given by Equation (S1-4). Thus $k_1 = \dfrac{1.667\Delta a}{\Delta\alpha\Delta T}$ is the approximate magnification factor of the NTEC. The first term in Equation (S1-6) can be neglected because its magnitude is much smaller than the second term. For given values of t/L, a/L and $\Delta\alpha\Delta T$, the magnification factor of the linear negative thermal expansion coefficient, k_1, can be obtained from Equations (S1-3), S1-4) and (S1-6).

For the first level 2D cellular materials with the geometrical structure shown in Figure 1d, the isotropic positive linear thermal expansion coefficient (PTEC) can be obtained in the similar manner and given as

$$\alpha_1 = \alpha_{RVE} = \frac{\Delta_{RVE}}{(1+2b)\Delta T} = \frac{\alpha_A + 2(b-a)\alpha_B}{1+2b} + \frac{2\Delta a}{(1+2b)\Delta T} \approx \frac{1.667\Delta a}{\Delta\alpha\Delta T}\Delta\alpha = k_1\Delta\alpha \qquad (S1\text{-}7)$$

Where the dimensionless $b = b/L$ is again chosen as 0.1. Similarly, the first level 2D cellular materials with the geometrical structure shown in Figure 1e have anisotropic linear thermal expansion coefficients of $k_1\Delta\alpha$ in one direction and $-k_1\Delta\alpha$ in the orthogonal direction.

For the first level 3D cellular materials with the geometrical structure of the representative volume element (i.e. RVE) shown in Figure 2a, the isotropic negative linear thermal expansion coefficient can be obtained as

$$\alpha_1 = \alpha_{RVE} = \frac{\Delta_{RVE}}{(1/\sqrt{2} + 2b)\Delta T} = \frac{\alpha_A + 2(b-a)\alpha_B}{1/\sqrt{2} + 2b} - \frac{2\Delta a}{(1/\sqrt{2} + 2b)\Delta T} \approx -\frac{2.205\Delta a}{\Delta\alpha\Delta T}\Delta\alpha = -k_1\Delta\alpha \quad \text{(S1-8)}$$

where Δa is given by Equation (S1-4).

Similarly, the isotropic positive linear thermal expansion coefficient of the first level 3D cellular materials with the geometrical structure given in Figure 2b and the anisotropic linear thermal expansion coefficient of the first level 3D cellular materials with the geometrical structure shown in Figure 2c can be derived as

$$\alpha_1 = \alpha_{RVE} = \frac{\Delta_{RVE}}{(1/\sqrt{2} + 2b)\Delta T} = \frac{\alpha_A + 2(b-a)\alpha_B}{1/\sqrt{2} + 2b} + \frac{2\Delta a}{(1/\sqrt{2} + 2b)\Delta T} \approx \frac{2.205\Delta a}{\Delta\alpha\Delta T}\Delta\alpha = k_1\Delta\alpha \quad \text{(S1-9)}$$

In Equations (S1-8) and (S1-9), the dimensionless dimension $b = b/L$ is also chosen as 0.1. Thus, the magnification factor of the positive, or negative, isotropic or anisotropic linear thermal expansion coefficient of the first level 3D cellular materials is $k_1 = \frac{2.205\Delta a}{\Delta\alpha\Delta T}$, which is 1.322 times that of the first level 2D cellular materials. Here, isotropic thermal expansion means that $(\alpha_{RVE})_x = (\alpha_{RVE})_y$ for 2D cellular materials and $(\alpha_{RVE})_x = (\alpha_{RVE})_y = (\alpha_{RVE})_z$ for 3D cellular materials.

Figure 4a shows the effects of the dimensionless amplitude a/L and the aspect ratio t/L of the chevron struts on the magnification factor k_1 of the positive or negative, isotropic or anisotropic linear thermal expansion coefficients of the first level 2D cellular materials with chevron struts which are pin-connected to the cross in the middle of the RVEs. It is noted that the magnitude of k_1 obtained from the above theoretical analysis is almost independent of the value of the relative thermal strain $\Delta\alpha\Delta T$ when $2\times10^{-6} \leq \Delta\alpha\Delta T \leq 0.02$. In addition, when a/L is smaller than 0.005, the magnitude of k_1 becomes smaller. This is because the ratio of $\varepsilon/(\Delta\alpha\Delta T)$ becomes larger with the reduction of a/L. We also found

that the transverse shear deformation of the chevron struts has negligible effect on the magnitude of the magnification factor k_1.

Figure 4a shows that when a/L is 0.005 and $t/L = 0.01$, the magnification factor k_1 of the first level 2D cellular materials is 41.75. The magnitudes of the linear isotropic or anisotropic NTEC or PTEC of the first level 2D cellular materials can thus reach $\alpha_1 = k_1 \Delta\alpha = 41.75 \times 2 \times 10^{-4} = 8.35 \times 10^{-3} \ K^{-1}$. This value is significantly larger than the positive or negative thermal expansion coefficients reported in references[3-8]. Moreover, if the ingredient B is chosen as a polyacrylamide material whose thermal expansion coefficient is $\alpha_B = -1.2 \times 10^{-3} \ K^{-1}$ (see reference[7]), the magnitude of the linear isotropic or anisotropic NTEC or PTEC of the first level 2D cellular materials could reach $\alpha_1 = k_1 \Delta\alpha = 41.75 \times 1.2 \times 10^{-3} = 5.01 \times 10^{-2} \ K^{-1}$, suggesting that the giant thermal expansion could be further improved by the thermal expansion coefficient of ingredient B.

It is noted that the derivation of the results in Figure 4a is independent of the Young's modulus of ingredient B as long as the deformation is linear elastic, as can be seen that E_B is absent in Equations (S1-3) and (S1-4). Although the transverse shear deformation of the chevron struts has negligible effect on the magnitude of k_1, the axial compression can significantly reduce the value of k_1. If without the effect of axial compression (i.e. if ε is zero in Equation (S1-4)), the magnification factor of the linear isotropic or anisotropic NTEC or PTEC of the first level 2D cellular materials would become $k_1 = \dfrac{1.667\Delta a}{\Delta\alpha\Delta T} = 1.667(a + \dfrac{L^2}{4a})$, which is independent of the aspect ratio t/L. In this case, $k_1 = 83.35$ if $a/L = 0.005$; and $k_1 = 41.68$ if $a/L = 0.01$, being much larger than those presented in Figure 4a.

S1.2. Nonlinear finite deformation analysis of chevron struts

The analysis in S1.1 and the results shown in Figure 4a are based on the initial undeformed configuration and obtained from the small deformation theory using a single Timoshenko beam element[32]. However, the thermal deformation of the chevron struts is in general a geometrical nonlinearity problem. The deformed configuration of half a chevron strut under thermal expansion and the restraint force P acted at the pin-jointed end is shown in Figure S1. The relationship between the bending curvature and the bending moment is given as [33, 34]

$$E_B I \frac{d\beta_b}{ds} = -Py = -\int_0^S P[(1+\Delta\alpha\Delta T - \frac{P}{E_B A}\cos\beta)\sin\beta]ds \qquad \text{(S1-10)}$$

Where the left hand side is the bending stiffness times the bending curvature and the right hand side is the bending moment. When $S = l = L/(2\cos\theta)$, $\beta_b(l) = \frac{\pi}{2} - \theta$ (see Figures 3a and S1), thus the angle $\beta_b(s)$ of the chevron strut due to the combined effects of strut bending, thermal expansion and axial compression can be determined as

$$\beta_b(s) = \frac{\pi}{2} - \theta + \frac{P}{E_B I}\int_s^l [\int_0^s (1+\Delta\alpha\Delta T - \frac{P}{E_B A}\cos\beta)\sin\beta ds]ds$$

$$= \frac{\pi}{2} - \theta + \frac{12\varepsilon_1}{t^2}\int_s^l [\int_0^s (1+\Delta\alpha\Delta T - \varepsilon_1\cos\beta)\sin\beta ds]ds \qquad \text{(S1-11)}$$

In the above equation, the strut is assumed to have a square cross-section of side t and

$$\varepsilon_1 = \frac{P}{E_B A} = \varepsilon/\cos\theta.$$

The angle due to transverse shear deformation of the strut is given as

$$\beta_S(s) = \frac{1.2P\sin\beta}{G_B A} = \frac{2.4(1+v_B)P}{E_B A}\sin\beta = 3.6\varepsilon_1\sin\beta \qquad \text{(S1-12)}$$

Where the Poisson ratio of the chevron material (i.e. a polymer) is chosen as 0.5.

The total angle of the deformed half chevron strut can thus be obtained as

$$\beta(s) = \beta_b(s) + \beta_S(s) \qquad \text{(S1-13)}$$

For a given value of the relative thermal strain $\Delta\alpha\Delta T$, the function $\beta(s)$ can be determined using the iterative method [33, 34] and the deformation compatibility condition:

$$\int_0^l (1+\Delta\alpha\Delta T - \varepsilon_1\cos\beta)\cos\beta\,ds = l\cos\theta = L/2 \qquad \text{(S1-14)}$$

To solve the nonlinear function $\beta(s)$, the length of half the chevron strut $l = L/(2\cos\theta)$ was divided into 100000 elements, the value of ε_1 was initially chosen as $\Delta\alpha\Delta T/2$ and $\beta(s)$ as θ. Using the iterative method, the convergent solution of $\beta(s)$ was very quickly obtained from the following solution scheme [33, 34]. The first step is to obtain new values of $\beta(s)$ using Equations (S1-11), (S1-12) and (S1-13), and the initially given or the already obtained values of ε_1 and $\beta(s)$. The second step is to check with the deformation compatibility condition (S1-14). In step 3, if the left hand side of Eq. (S1-14) is larger than the right hand side, it suggests that the value of ε_1 is too small, then increase the value of ε_1; if the left hand side of Eq. (S1-14) is smaller than the right hand side, it suggests that the value of ε_1 is too large, then reduce the value of ε_1. Step 4 is to check the new values of $\beta(s)$ with the previous values, if the largest difference is smaller than 10^{-6}, convergent solution of $\beta(s)$

has been obtained; otherwise repeat steps 1-4 using the updated values of ε_1 and $\beta(s)$.

Thus very accurate solution of $\beta(s)$ can be very quickly obtained for any given value of the

relative thermal strain $\Delta\alpha\Delta T$, and the change of the amplitude of the chevron strut, Δa, can

be obtained as

$$\Delta a = \int_0^l (1 + \Delta\alpha\Delta T - \varepsilon_1 \cos\beta)\sin\beta\, ds - a \tag{S1-15}$$

It is noted that in the analysis of S1.1 and S1.2, the combined effects of thermal expansion,

bending, axial compression and transverse shear on the thermal deformation of the chevron

struts are all considered. The thermal expansion magnification factor of the 2D and 3D

cellular materials can be obtained using the relevant equations given in section S1.1.

S1.3. Deformation analysis of pin-jointed struts

If the chevron strut in Figure 3a is replaced by two pin-jointed struts as shown in Figure 3b,

for a given value of the relative thermal expansion $\Delta\alpha\Delta T$, the change of the amplitude in

Figure 3b can be obtained as

$$\Delta a = \sqrt{(L^2/4 + a^2)(1 + \Delta\alpha\Delta T)^2 - L^2/4} - a \tag{S1-16}$$

and the values of the thermal expansion magnification factor k_1 of the 2D cellular materials

can be obtained using the relevant equations given in section S1.1, and presented in Figure 4b

for 2D cellular materials. For the first level 3D cellular materials with pin-jointed struts, the

values of the thermal expansion magnification factor are 1.322 times those of their 2D

counterparts.

S1.4. Validation by finite element simulation

To verify the theoretical results given in Figures 4a and 4b for the first level 2D cellular materials, we have performed finite element simulation using the commercial software ABAQUS. Half a chevron strut is partitioned into 800 plane stress CPS4T elements and the obtained results are shown in Tables S1 and S2 to validate the theoretical results of Figures 4a and 4b. For the cases when the chevron struts are pin-jointed with the cross, the FEM results in Table S1 show quite good agreement with theoretical results although the FEM results indicate that the larger the value of $\Delta\alpha\Delta T$, the smaller the magnification factor k_1. For the cases when the chevron struts are replaced by two pin-jointed struts, the FEM results in Table S2 are identical to the theoretical results.

S1.5. Thermal expansion coefficient of hierarchical and self-similar cellular materials

For the nth level hierarchical and self-similar 2D cellular materials shown in Figure 1, the thermal expansion coefficient can be obtained as

$$\alpha_n = \Delta\alpha \cdot (k_1)^n = (\alpha_B - \alpha_A)(k_1)^n \tag{S1-17}$$

if the shape of the RVE is convex, and

$$\alpha_n = \Delta\alpha \cdot (-k_1)^n = (\alpha_B - \alpha_A)(-k_1)^n \tag{S1-18}$$

if the shape of the RVE is concave.

For the nth level hierarchical and self-similar 3D cellular materials, the thermal expansion coefficient can be obtained as $\alpha_n = \Delta\alpha \cdot (1.322k_1)^n = (\alpha_B - \alpha_A) \cdot (1.322k_1)^n$ if the shape of the RVE is convex, and $\alpha_n = \Delta\alpha \cdot (-1.322k_1)^n = (\alpha_B - \alpha_A) \cdot (-1.322k_1)^n$ if the shape of the RVE is concave.

S2. The stiffness of 2D and 3D cellular materials

When a uniaxial tensile stress σ_x is applied to the RVEs of the first level 2D cellular materials with chevron struts, as shown in Figures 1c, 1d and 1e, the concentrated force applied at the vertex of the chevron strut on the left hand side or right hand side is $F = \sigma_x(L + 2b) = 1.2L\sigma_x$, where $b = 0.1L$.   The chevron struts can be treated as pin-supported beams with a span of L and the horizontal deformation of the RVEs can thus be approximated as $\Delta_x = \dfrac{2FL^3}{48E_BI} = \dfrac{0.6\sigma_xL^4}{E_Bt^3}$ where $I = \dfrac{t^3}{12}$.   This is because bending of the chevron struts is the dominant deformation mechanism. The horizontal strain can be derived as $\varepsilon_x = \Delta_x/(L + 2b) = \Delta_x/(1.2L) = \sigma_xL^3/(2E_Bt^3)$.   Thus the Young's modulus of the first level 2D cellular materials is obtained as

$$E_1 = \frac{\sigma_x}{\varepsilon_x} = 2(\frac{t}{L})^3 E_B \tag{S2-1}$$

For the nth level hierarchical and self-similar 2D cellular materials, the Young's modulus can be obtained in the similar manner, and given as

$$E_n = 2(\frac{t}{L})^3 E_{n-1} = 2^n (\frac{t}{L})^{3n} E_B \tag{S2-2}$$

Similarly, the Young's modulus of the first level 3D cellular materials with pin-jointed chevron struts can be obtained as

$$E_1 = \frac{\sigma_x}{\varepsilon_x} = \frac{4t^4E_B}{(\sqrt{2}L/2 + 2b)L^3} = 4.41(\frac{t}{L})^4 E_B \tag{S2-3}$$

For the nth level hierarchical and self-similar 3D cellular materials, the Young's modulus is obtained as

$$E_n = 4.41(\frac{t}{L})^4 E_{n-1} = 4.41^n (\frac{t}{L})^{4n} E_B \tag{S2-4}$$

If the chevron strut in Figure 3a is replaced by two pin-jointed struts with a uniform thickness t for 2D cellular materials, as shown in Figure 3b, when a uniaxial tensile stress σ_x is applied to the RVEs of the first level 2D cellular materials, as shown in Figures 1c, 1d and

1e, the axial tensile force in each of the two pin-jointed struts is $N = \dfrac{\sigma_x(L+2b)}{2\sin\theta}$ and the

elongation of the struts is $\Delta = \dfrac{NL}{2E_B t \cos\theta} = \dfrac{\sigma_x L(L+2b)}{4tE_B \sin\theta\cos\theta}$. Thus the tensile strain of the 2D

RVE in the x direction is $\varepsilon_x = \dfrac{2\Delta}{(L+2b)\sin\theta} = \dfrac{\sigma_x L}{2E_B t \sin^2\theta\cos\theta}$, and the Young's modulus of

the first level 2D cellular materials is obtained as

$$E_1 = \frac{\sigma_x}{\varepsilon_x} = \frac{2E_B t \sin^2\theta\cos\theta}{L} = \frac{8ta^2}{(L^2+4a^2)^{3/2}}E_B \tag{S2-5}$$

For the nth level hierarchical and self-similar 2D cellular materials, the Young's modulus can be obtained in the similar manner, and given as

$$E_n = \frac{8ta^2}{(L^2+4a^2)^{3/2}}E_{n-1} = \frac{(8ta^2)^n}{(L^2+4a^2)^{3n/2}}E_B \tag{S2-6}$$

Similarly, the Young's modulus of the first level 3D cellular materials is obtained as

$$E_1 = \frac{\sigma_x}{\varepsilon_x} = \frac{t^2a^2 E_B}{(L^2/4+a^2)^{3/2}(\sqrt{2}L/4+b)} = \frac{17.64t^2a^2}{(L^2+4a^2)^{3/2}}E_B \tag{S2-7}$$

where $b = 0.1L = 0.1$ $b = 0.1L = 0.1$.

For the nth level hierarchical and self-similar 3D cellular materials, the Young's modulus can be obtained as

$$E_n = \frac{(17.64t^2a^2)^n}{(L^2+4a^2)^{3n/2}}E_B \tag{S2-8}$$

References

[31] J.N. Grima, R. Gatt, A. Alderson, K.E. Evans, *Molecular Simulation.* **2005**, 31, 925.

[32] J.M. Gere, S.P. Timoshenko, Mechanics of Materials, Cambridge University Press, 1985.

[33] H.X. Zhu, N.J. Mills, *Int. J. Solids and Struct.* **2000**, 37, 1931.

[34] H.X. Zhu, N.J Mills, J.F. Knott, *J. Mech. Phys. Solids* **1997**, 45, 1875.
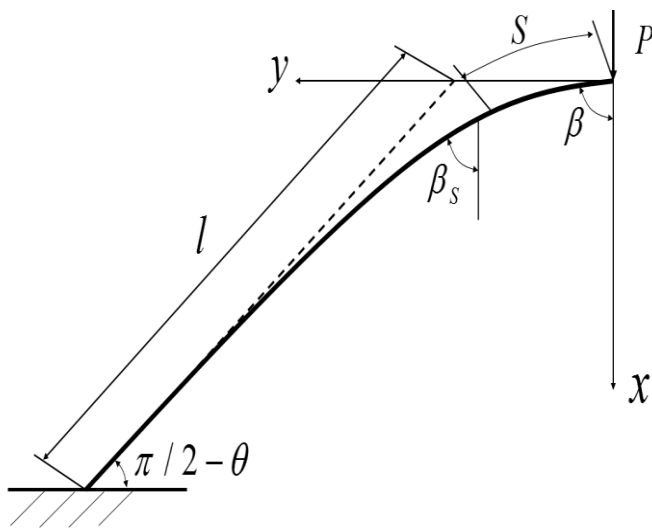
Figure

Figure S1. The deformed half chevron strut under thermal expansion and restraint force P.

Table S1. FEM validation for results presented in Figure 4a.

t/L	a/L	ΔT (K)	k_1 (theoretical result)	k_1 (FEM result)

0.01	0.005	1	41.763	40.225
0.01	0.005	1.5	41.763	37.512
0.025	0.05	5	7.943	7.578
0.025	0.05	25	7.943	6.594
0.045	0.05	0.5	7.028	6.9015
0.045	0.05	5	7.028	6.7612

Table S2.   FEM validation for results presented in Figure 4b.

a/L	ΔT (K)	k_1 (Theoretical result)	k_1 (FEM result)
0.001	0.005	374.58	374.658
0.001	0.5	102.36	102.38
0.001	5	35.648	35.662
0.05	0.5	8.375	8.376
0.05	5	8.034	8.035
0.08	5	5.2431	5.243
0.1	5	4.2805	4.2806